Neuro-Oncology

Neuro-Oncology 18(9), 1265–1277, 2016
doi:10.1093/neuonc/now032
Advance Access date 6 March 2016

Components of the eIF4F complex are potential therapeutic targets for malignant peripheral nerve sheath tumors and vestibular schwannomas

Janet L. Oblinger, Sarah S. Burns, Elena M. Akhmametyeva, Jie Huang, Li Pan, Yulin Ren, Rulong Shen, Beth Miles-Markley, Aaron C. Moberly, A. Douglas Kinghorn, D. Bradley Welling†, and Long-Sheng Chang

Center for Childhood Cancer and Blood Diseases, The Research Institute at Nationwide Children's Hospital and Department of Pediatrics, The Ohio State University College of Medicine, Columbus, Ohio (J.L.O, S.S.B, E.M.A, J.H., L.-S.C.); Department of Otolaryngology-Head and Neck Surgery, The Ohio State University College of Medicine, Columbus, Ohio (J.L.O, S.S.B, B.M.M, A.C.M, D.B.W, L.-S.C.); Department of Pathology, The Ohio State University College of Medicine, Columbus, Ohio (R.S., L.-S.C.); Division of Medicinal Chemistry and Pharmacognosy, The Ohio State University College of Pharmacy, Columbus, Ohio (L.P., Y.R., A.D.K.)

Corresponding Author: Long-Sheng Chang, PhD, Center for Childhood Cancer and Blood Diseases, Nationwide Children's Hospital, 700 Children's Drive, Columbus, OH 43205 (lchang@chi.osu.edu).

†Present Address: Department of Otology and Laryngology, Harvard Medical School and Massachusetts Eye and Ear Infirmary, Massachusetts General Hospital, 243 Charles Street, Boston, MA 02114.

Background. The eukaryotic initiation factor 4F (eIF4F) complex plays a pivotal role in protein translation initiation; however, its importance in malignant and benign Schwann cell tumors has not been explored, and whether blocking eIF4F function is effective for treating these tumors is not known.

Methods. Immunostaining was performed on human malignant peripheral nerve sheath tumors (MPNSTs) and vestibular schwannomas (VSs) for eIF4F components. The role of eIF4A and eIF4E in cell growth was assessed by RNA interference. Various natural compounds were screened for their growth-inhibitory activity. Flow cytometry and Western blotting were performed to characterize the action of silvestrol, and its antitumor activity was verified in orthotopic mouse models.

Results. MPNSTs and VSs frequently overexpressed eIF4A, eIF4E, and/or eIF4G. Depletion of eIF4A1, eIF4A2, and eIF4E substantially reduced MPNST cell growth. From screening a panel of plant-derived compounds, the eIF4A inhibitor silvestrol was identified as a leading agent with nanomolar IC_{50} values in MPNST and VS cells. Silvestrol induced G_2/M arrest in both *NF1*-deficient and *NF1*-expressing MPNST cells and primary VS cells. Silvestrol consistently decreased the levels of multiple cyclins, Aurora A, and mitogenic kinases AKT and ERKs. Silvestrol treatment dramatically suppressed tumor growth in mouse models for $NF1^{-/-}$ MPNST and $Nf2^{-/-}$ schwannoma. This decreased tumor growth was accompanied by elevated phospho-histone H3 and TUNEL labeling, consistent with G_2/M arrest and apoptosis in silvestrol-treated tumor cells.

Conclusions. The eIF4F complex is a potential therapeutic target in MPNSTs and VS, and silvestrol may be a promising agent for treating these tumors.

Keywords: eIF4F complex, malignant peripheral nerve sheath tumor (MPNST), orthotopic mouse models, silvestrol, vestibular schwannoma (VS).

Translation initiation is the key rate-limiting step for protein biosynthesis and involves recruitment of the eukaryotic initiation factor 4F (eIF4F) complex to the 5′ cap of mRNA.[1] This complex is composed of eIF4E, which binds the 5′ cap, eIF4A, an RNA helicase that unwinds the secondary structure of the 5′ region of mRNA, and eIF4G, which functions as a scaffold for other eIFs and enhances the helicase activity of eIF4A. Studies have suggested that oncogenesis is driven by uncontrolled protein translation. Constitutive activation of oncogenic kinases (eg, AKT, mTOR and ERK1/2) are frequently activated in human tumors. These kinases inhibit the 4E-BP translational repressors, facilitating eIF4F assembly and leading to elevated protein synthesis.[2] Also, AKT and ERK phosphorylate eIF4B, thereby increasing eIF4A's helicase activity. In addition, overexpression of

Received 2 November 2015; accepted 6 February 2016

eIF4F components frequently occurs during tumorigenesis. High levels of eIF4E are observed in several cancer types and often correlate with tumor grade, metastasis, and poor survival.[3] While the expression status of eIF4G and eIF4A has been less well-characterized, amplification of eIF4G has been reported in squamous lung carcinomas.[2] Of the 2 members of eIF4A that can form the eIF4F complex, increased eIF4A1 expression has been found in liver, cervical, and breast cancers.[2,4] Additionally, the enforced expression of eIF4A accelerates leukemogenesis.[5]

AKT and ERK1/2 are commonly activated in malignant peripheral nerve sheath tumors (MPNSTs) and their activation is important for tumor growth. MPNSTs are aggressive tumors that arise along peripheral nerves and are primarily composed of neoplastic Schwann cells.[6] With no effective treatment currently available, patients with MPNSTs have a poor 5-year survival of only 20∼50%. MPNSTs occur sporadically or as part of the genetic syndrome neurofibromatosis type 1 (NF1), which is caused by mutations in the *NF1*/neurofibromin gene.[7] The mutational loss of *NF1* constitutively activates the Ras pathway, resulting in deregulated PI3K/AKT/mTOR and ERK signaling. The *NF1*-associated MPNSTs often develop in association with a preexisting benign plexiform neurofibroma, representing malignant transformation of benign tumor cells.[8] Sporadic MPNSTs likewise exhibit elevated ERK and AKT signaling due to multiple genetic lesions such as *EGFR* amplification and *PTEN* loss.[6]

Activated AKT and ERK1/2 also drive the growth of benign Schwann cell tumors, vestibular schwannomas (VSs), which cause significant morbidities such as hearing loss, facial nerve paralysis, brainstem compression, hydrocephalus, and death. VS can occur sporadically or in patients with NF2, which is caused by inactivation of the *NF2*/merlin gene.[9,10] The loss of merlin function results in the abnormal activation of receptor tyrosine kinases (RTKs) and PI3K. Consequently, these tumors have high levels of activated AKT and ERKs.[11] Merlin has also been reported to associate with and inhibit eIF3c, suggesting a link to the control of protein translation.[12] An FDA-approved medical therapy is not currently available for the treatment of VS. As activation of AKT and ERK in VS and MPNSTs can drive enhanced protein translation, inhibiting the protein translational machinery might be a viable means for treating these tumors.

Recently, the eIF4A inhibitor silvestrol has received considerable attention since it possesses a nanomolar cytotoxic potency against hematological malignancies, colorectal carcinoma, and hepatocellular carcinoma.[13–17] It also exhibits an overall favorable pharmacokinetic profile in mice[18] and has been under preclinical evaluation in the NCI Experimental Therapeutics (NExT) Program (http://next.cancer.gov/about/pipeline_preclinical.htm; last access 29 February 2016). Silvestrol binds to and inhibits eIF4A1/2, preventing the formation of the eIF4F complex[19–21]; however, the antitumor effects of silvestrol in MPNSTs and VS have not been investigated.

In this study, we demonstrated frequent overexpression of eIF4F components in MPNSTs and VS and identified silvestrol from a natural compound screen as the most potent growth-inhibitory agent in both tumors. Silvestrol causes G_2/M arrest and reduces several cyclins and key signaling kinases. Significantly, it efficiently inhibits tumor growth and induces apoptosis in orthotopic *NF1*$^{-/-}$ MPNST and *Nf2*$^{-/-}$ schwannoma animal models.

Materials and Methods

Tissue Acquisition and Cell Cultures

The Ohio State University IRB approved the human subject protocols for the acquisition of normal nerves and tumor specimens after informed patient consent. Primary VS and Schwann cells were prepared and propagated as previously described.[22] ST8814 and STS26T MPNST and luciferase-expressing ST8814-Luc and Sch10545-Luc cells were grown in Dulbecco's modified Eagle's medium (DMEM) containing 10% fetal bovine serum. More details are found in Supplementary Methods.

Lentiviral-mediated Short-hairpin RNA Knockdown

MPNST cells were plated in 6-well plates at 9000 cells/well. The following day, cells were fed with fresh medium containing 8 μg/mL polybrene and infected with MISSION short-hairpin (sh)RNA lentiviral particles (Sigma) targeting *EIF4A1*, *EIF4A2*, *EIF4E* (Supplementary Table S1), or a non-targeting control (#SHC002V) at a multiplicity of infection (MOI) of 10. Two days later, transduced cells were selected with 2.5 μg/mL puromycin for 6–7 days prior to cell counting and Western blotting. Densitometric analysis of the protein band intensities was performed using ImageJ (http://rsb.info.nih.gov/ij/index.html; last access 29 February 2016) and computed as a percentage of the nontargeting control after normalizing to α-tubulin or GAPDH.

Natural Compound Treatment, Cell Proliferation Assays, and Flow Cytometry

A panel of 23 natural compounds (Supplementary Table S2) was purified as part of a multi-institutional program for the discovery of new anticancer agents from plants, and their full structures and absolute configurations were established.[15,23] Purified compounds were dissolved to 1∼10 mM stocks in dimethylsulfoxide (DMSO). To evaluate the antiproliferative effects of these compounds, cells were seeded in 96-well plates at 4000 cells/well except for primary VS and Schwann cells (10 000 cells/well). The following day, cells were treated with various concentrations of each compound or DMSO as a control. After 3 days, cell proliferation was assessed, and the IC_{50} value was calculated.[24] Cell cycle analysis was performed accordingly[24] (Supplementary Methods).

Orthotopic Animal Models, Bioluminescence Imaging, and Magnetic Resonance Imaging

The Institutional Animal Care and Use Committee at Nationwide Children's Hospital approved this animal study. Under anesthesia, blunt dissection of the biceps femoris was used to localize the sciatic nerves,[25] which were injected with 2×10^4 ST8814-Luc or 1×10^6 Sch10545-Luc cells using a Hamilton Neuros syringe attached with a 33-gauge needle. Following tumor establishment,[24] mice were randomized into 2 groups ($n = 6$ each) and were treated with either 1.5 mg/kg of silvestrol or 30% hydroxypropyl-β-cyclodextrin (HPβCD) as the vehicle control by i.p. injection (every other day). Tumor growth was monitored weekly by bioluminescence imaging (BLI) using a Xenogen IVIS Spectrum (Caliper).[24] Also, tumor xenografts

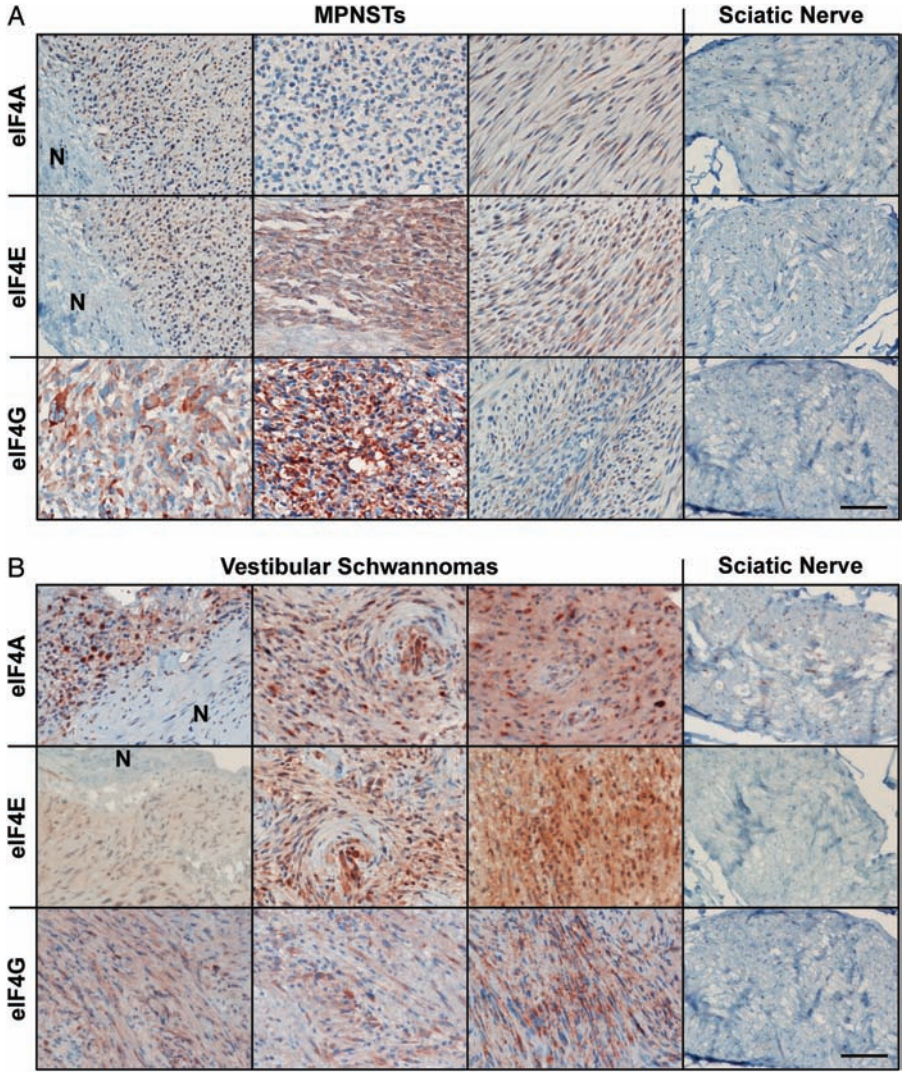

Fig. 1. Malignant peripheral nerve sheath tumors (MPNSTs) and vestibular schwannomas (VSs) overexpress all 3 eIF4F components. Shown are representative images for MPNST (A) and VS (B) sections immunostained for eIF4A, eIF4E and eIF4G. "N" indicates adjacent normal nerve tissues. Immunostaining of normal sciatic nerve sections served as controls. The relative staining signals from all samples are summarized in Supplementary Table S3. Scale bar is 200 μm. For high-magnification images, see Supplementary Fig. S1.

were imaged by MRI at the beginning and end of the experiment, and tumor volumes were computed from T1-weighted images.[11,26]

Western Blots and Immunohistochemistry

Subconfluent cells were treated with the indicated doses of silvestrol for 24 hours and then lysed in Laemmli buffer containing 2% SDS. Normal nerve and VS tissues were homogenized in lysis buffer using pellet pestles (Kontes). The total protein content in cleared lysates was quantitated using the microBCA assay (Thermo). Equal amounts of protein were resolved by SDS-polyacrylamide gel electrophoresis and transferred to polyvinylidene difluoride membranes.

Normal human nerve, MPNST, and VS tissue sections were processed and immunostained as described previously.[24] Also, following the last imaging session, ST8814-Luc and Sch10545-Luc tumors in mice with or without silvestrol treatment were harvested and stained with hematoxylin and eosin (H&E) or immunostained for p-histone H3(Ser^{10}) (Abcam) or TUNEL using the TMR Red *In Situ* Cell Death Detection Kit (Roche). Further details for Western blots and immunohistochemistry (IHC) are found in Supplementary Methods.

Statistical Analysis

The Fisher exact test was used to determine if the staining intensities of eIF4A, eIF4E, or eIF4G within VS specimens differed between solid and cystic tumors or between sporadic and NF2 diagnoses. A similar analysis was performed for MPNST specimens for sporadic versus NF1 tumors. Two-tailed Student *t* tests were used to determine the statistical significance of growth inhibition following eIF4A and eIF4E depletion in MPNST cells.

Table 1. Summary of relative IHC staining signals for eIF4A, eIF4E, and eIF4G in normal sciatic nerves, MPNSTs, and vestibular schwannomas. Tissue sections were processed by immunohistochemistry analysis as described in Materials and Methods. Quantification of immunostaining signal was performed by visual analysis on a 0 to 3+ scale (0 as negative, 0.5+ as weak positive, 1+ as moderate positive, 2+ as strong positive, and 3+ as very strong positive) based on the intensity and percentage of immunopositive cells and their subcellular compartmentalization

Tissue/Tumor	ID No.	eIF4A	eIF4E	eIF4G
Sciatic nerve	1	0 (rare 0.5+)	0	0
	2	0 (occasional 0.5+)	0	0
MPNST	M1	1 ~ 2 +	2 +	3 +
	M2	0 ~ 0.5 +	0 ~ 1 +	0 ~ 1 +
	M3	1 ~ 2 +	2 ~ 3 +	0 ~ 1 +
	M4	Rare 1+ (mostly necrosis)	0 (necrotic tissue)	0 (necrotic tissue)
	M5	1 +	2 ~ 3 +	1 ~ 2 +
	M6	0 ~ 0.5 +	1 +	3 +
	M7	0.5 ~ 1 +	1 +	0 ~ 1 +
	M8	0 (occasional 0.5+)	0	0
	M9	0 with patchy 1 +	0.5 ~ 1 +	1 ~ 3 +
	M10	1+ with patchy 2 +	1 ~ 2 +	3 +
	M11	1 ~ 2 +	0	0 ~ 0.5 +
	M12	0 ~ 1 +	0 ~ 1 +	1 ~ 2 +
	M13	1 ~ 3 +	1 +	3 +
	M14	0 ~ 0.5 +	1 +	3 +
	M15	1 ~ 2 +	3 +	1 +
	M16	1 ~ 2 +	3+ with patchy 2 +	3 +
	M17	0.5 ~ 1 +	1+ with patchy 2 +	Patchy 3 +
	M18	0 ~ 0.5 +	0.5 ~ 1 +	1+ with patchy 2 +
	M19	0 ~ 0.5 +	1 ~ 1.5 +	0 ~ 0.5 +
Vestibular schwannoma	VS1	0 with patchy 2 +	0 ~ 1 +	1 +
	VS2	2 +	2 ~ 3 +	1 ~ 2 +
	VS3	2 ~ 3 +	2+ with patchy 3 +	1 +
	VS4	2 ~ 3 +	1+ with patchy 2 +	1 +
	VS5	1 +	1 +	1 +
	VS6	1 ~ 2 +	3 +	ND
	VS7	2 ~ 3 +	3 +	1 ~ 2 +
	VS8	1 +	3 +	1+ with patchy 2 +
	VS9	1 +	0.5 ~ 1+	2 +
	VS10	3 +	3 +	1 ~ 1.5 +
	VS11	3 +	3 +	1 ~ 2 +
	VS12	3 +	3 +	0.5 ~ 1 +
	VS13	1+ with patchy 3 +	3 +	0.5 ~ 1 +
	VS14	1 ~ 2 +	1 +	1 +
	VS15	2 ~ 3 +	3 +	2 +
	VS16	1 ~ 2 +	2 ~ 3 +	2 +
	VS17	3 +	1 ~ 2 +	1 +
	VS18	2 ~ 3 +	1 +	0 with patchy 2 +
	VS19	2 ~ 3 +	2+ with patchy 3 +	0 with patchy 1 +
	VS20	2 ~ 3 +	1 ~ 2 +	ND

Results

Malignant Peripheral Nerve Sheath Tumors and Vestibular Schwannomas Frequently Overexpress the Components of the eIF4F Complex

To examine the expression levels of eIF4F components, we immunostained tissue sections of 19 MPNST, 20 VSs, and 2 normal nerve specimens for eIF4A, eIF4E, and eIF4G. The majority of MPNSTs showed more intense labeling of all 3 eIF4F components than normal nerve tissues, which had only barely detectable labeling (Fig. 1A and Supplementary Table S3). Prominent eIF4A staining was detected in the cytoplasm of MPNST cells and was particularly concentrated at specific locations near the nucleus, suggesting localization to the rough endoplasmic reticulum (Supplementary Fig. S1A). Consistent with its functions in protein translation

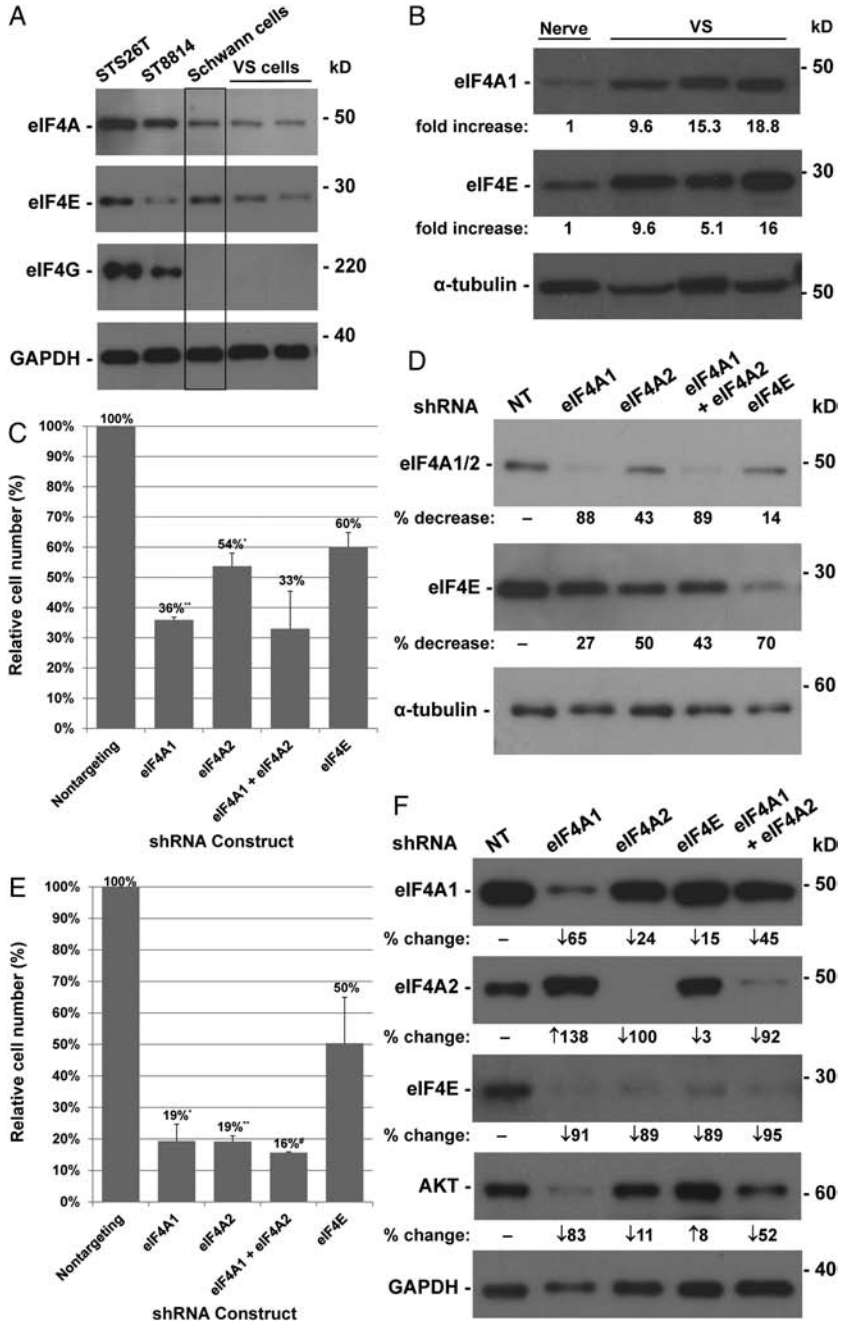

Fig. 2. Depletion of eIF4A and eIF4E inhibits proliferation of STS26T and ST8814 malignant peripheral nerve sheath tumor (MPNST) cells. Western blotting of protein lysates prepared from STS26T and ST8814 MPNST cells and primary vestibular schwannomas (VSs) and Schwann cells (A) and from normal nerve and VS tissues (B) was performed and probed for various eIF4F components. GAPDH or α-tubulin served as a loading control. Densitometry was used to estimate the fold-difference in protein expression between VS and normal nerve tissues. (C) STS26T cells were transduced with 10 MOI of the indicated lentiviral shRNA vectors, selected with puromycin, and counted. Shown are % cell numbers relative to the nontargeting (NT) control designated as 100%. Means and SDs were calculated from 2 independent experiments. (D) Following counting, cells were lysed, and equal amounts of protein lysates were probed for eIF4A1/2, eIF4E, and α-tubulin. The % decrease in eIF4A or eIF4E protein levels in the indicated shRNA-transduced cells versus NT controls is shown. (E) ST8814 cells were transduced with the indicated lentiviral shRNA vectors and counted after puromycin selection. (F) Protein lysates from transduced cells were probed for various eIF4F components and AKT. Statistics for cell counting in (C) and (E) were performed using the 2-sample *t* test assuming unequal variances ($^{*}P < .05$, $^{**}P = .01$, $^{\#}P = .001$ vs NT controls).

and mRNA export,[27] eIF4E exhibited both cytoplasmic and nuclear localization with concentrated perinuclear staining. While the labeling for eIF4G appeared more diffuse throughout the cytoplasm, concentrated staining around the nucleus was also seen. Notably, 8 out of the 19 MPNSTs analyzed showed intense (3+) eIF4G staining.

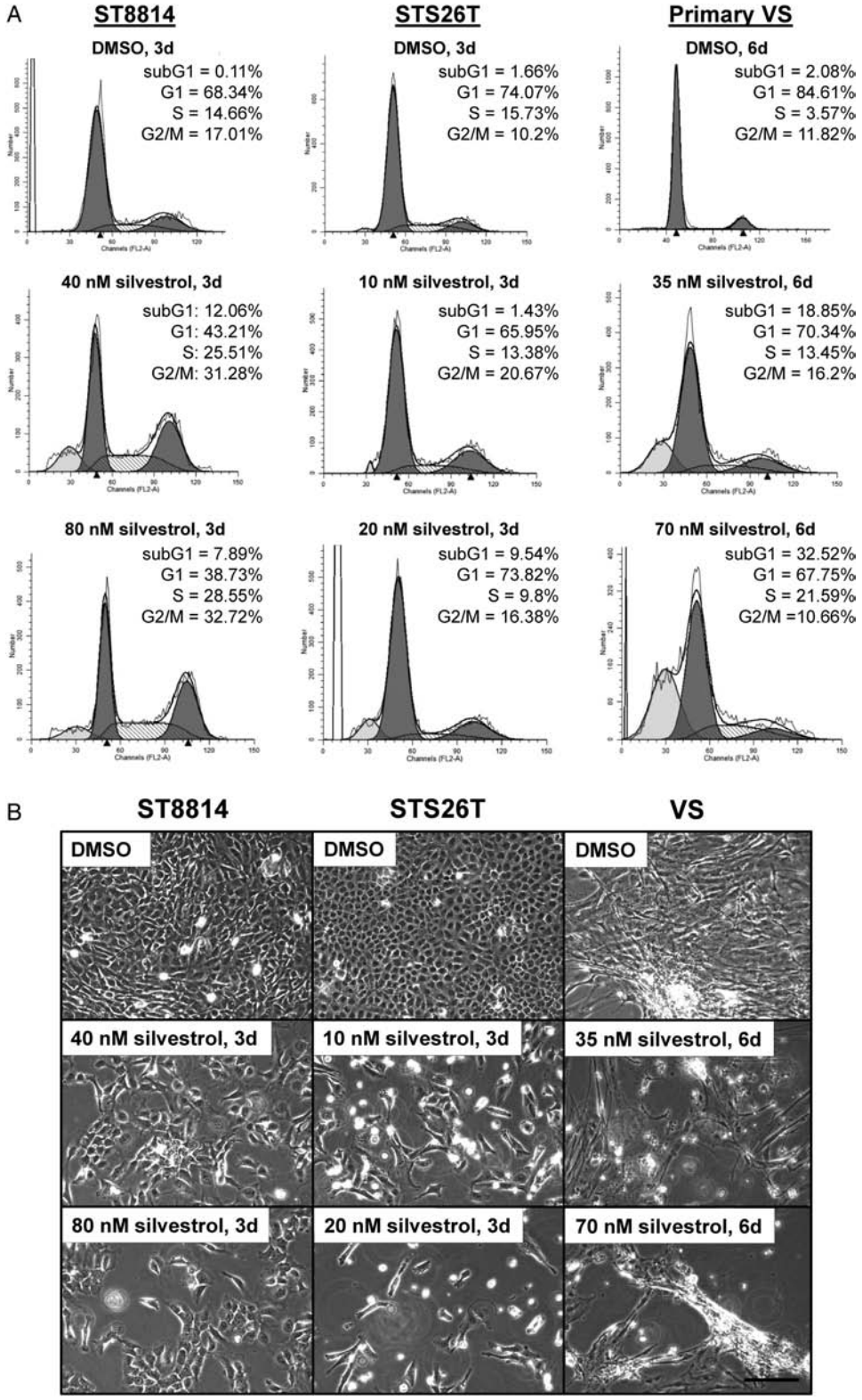

Fig. 3. Silvestrol promotes G_2/M arrest in malignant peripheral nerve sheath tumors (MPNSTs) and vestibular schwannoma (VS) cells. (A) Histograms of propidium iodide-labeled ST8814 and STS26T MPNST and primary VS cells reveal an increased proportion of cells in G_2/M after silvestrol treatment for the indicated days (d). Also, silvestrol-treated cells exhibited an increase in the sub-G_1 fraction, indicative of cell death. (B) Phase contrast micrographs showed that MPNST and VS cells treated with the indicated concentrations of silvestrol manifested debris and floating cells, consistent with cell death. Scale bar is 200 μm.

Similarly, VS specimens displayed stronger labeling for all 3 eIF4F components than normal nerve tissues (Fig. 1B and Supplementary Table S3). Intriguingly, the majority (12/20) of VSs examined showed very strong (3+) eIF4A staining in the cytoplasm with high concentrations at perinuclear locations (Supplementary Fig. S1B). Also, most (12/20) VSs exhibited very strong cytoplasmic staining of eIF4E. While the staining pattern was more diffused compared with that of eIF4A, perinuclear localization of eIF4E was still observed. In addition, moderate-to-strong eIF4G staining was detected in most VSs.

To corroborate the IHC findings, we compared the protein levels of eIF4A, eIF4E, and eIF4G in 2 human MPNST cell lines (*NF1*$^{-/-}$ ST8814 and *NF1*$^{+/+}$ STS26T) and 2 primary cultures of VS cells from different patients with those in primary human Schwann cells. Both MPNST cell lines expressed higher levels of eIF4A and eIF4G than cultured Schwann cells (Fig. 2A). While the eIF4E expression level in STS26T cells was comparable to or slightly higher than that in Schwann cells, it was slightly lower in ST8814 cells. Unexpectedly, we found that primary VS cells expressed all 3 eIF4F components at levels similar to those in Schwann cells (Fig. 2A). It is possible that the growth factor-rich conditions enable cultured Schwann cells to express more eIF4F components to promote higher protein synthesis for growth. To test this possibility, we directly compared the expression levels of eIF4A and eIF4E in VSs and normal vestibular nerve tissues. As shown in Fig. 2B, all 3 VS tumors examined had higher expression of eIF4A1 (~14-fold) and eIF4E (5–16-fold) compared with normal nerve. These results indicate that both MPNSTs and VSs frequently overexpress eIF4F components.

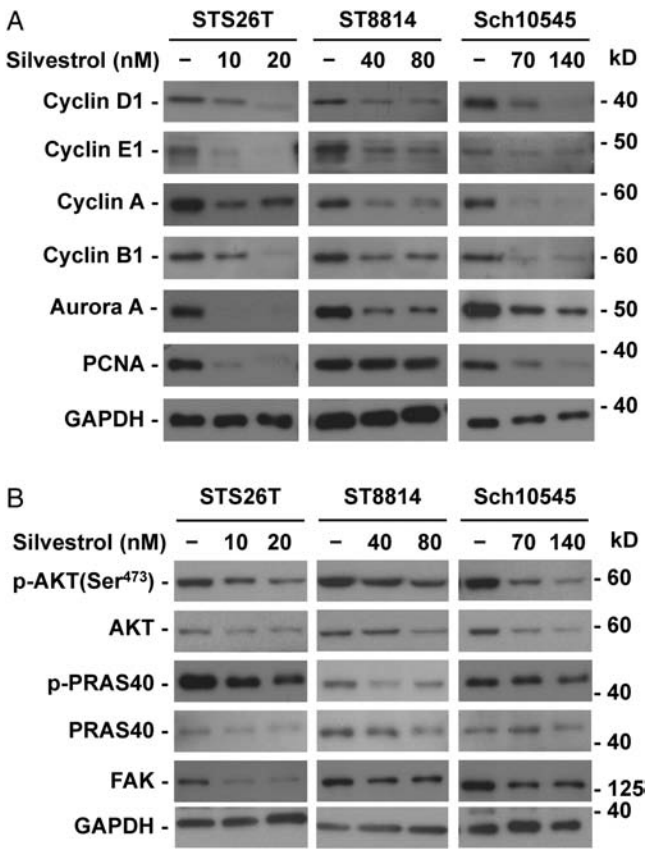

Fig. 4. Silvestrol inhibits the expression of multiple cyclins and kinases. ST8814 and STS26T malignant peripheral nerve sheath tumor (MPNST) and Sch10545 schwannoma cells treated with 1x and 2x the IC_{50} dose of silvestrol for 24 hours were analyzed by Western blots for the expression of various cyclin, Aurora A, and PCNA proteins (A) and total and phosphorylated AKT and its downstream substrate PRAS40 as well as FAK (B). GAPDH served as a loading control.

The high eIF4E expression is associated with malignant progression and poor prognosis in several types of cancers.[3] Increased eIF4A levels also correlate with poor survival in estrogen receptor-negative breast cancer.[4] Thus, we determined whether the expression levels of the eIF4F components correlated with clinicopathological parameters in MPNSTs and VS. Of the 19 MPNST specimens analyzed, expression of eIF4A, eIF4E, or eIF4G did not appear to correlate with tumor grade, recurrence, or patient age (Table 1 and Supplementary Table S4). However, NF1-associated MPNSTs tended to exhibit stronger eIF4G staining than sporadic tumors. Among the 20 VS tumors, all 4 NF2-associated tumors had very strong labeling for eIF4A (Table 1 and Supplementary Table S5). The 7 cystic VS tumors, all larger in size compared with the solid tumors analyzed, also frequently showed strong staining for eIF4A ($n = 5/7$) and eIF4E ($n = 6/7$). These associations, while interesting, did not reach statistical significance due to the small sample size ($P = .6063$ and $P = .4044$, respectively). Nonetheless, frequent overexpression of eIF4F components in VS and MPNSTs suggests the importance of this eIF4F complex in the growth of these tumors.

Knockdown of eIF4A and eIF4E Reduces MPNST Cell Growth

To determine the role of eIF4F components in cell proliferation, we used lentiviral-mediated shRNAs to deplete eIF4A1, eIF4A2, and eIF4E in MPNST cells. Consistent with knockdown efficiencies, shRNAs targeting eIF4A1, eIF4A2, or eIF4E substantially reduced *NF1*$^{+}$ STS26T cell growth relative to the nontargeting control (Fig. 2C and D). Proliferation of *NF1*-deficient ST8814 cells was even more profoundly inhibited by these shRNAs: depletion of eIF4E halved cell growth, and silencing of eIF4A1 or eIF4A2 reduced cell numbers >80% (Fig. 2E). Intriguingly, eIF4A1 depletion in ST8814 cells induced an increase in eIF4A2 protein (Fig. 2F); however, this increase was unable to rescue cell proliferation (Fig. 2E). Also, silencing eIF4A1 and eIF4A2 resulted in reduced eIF4E expression, particularly in ST8814 cells (Fig. 2F). This associated decrease in eIF4E by depletion of eIF4A1 and eIF4A2 may augment the antiproliferative effects of these shRNAs (Fig. 2E). ST8814 cells also showed decreased AKT levels after eIF4A1 depletion. Overall, our results suggest that high levels of eIF4A and eIF4E are important for MPNST cell growth, and that both eIF4A1 and eIF4A2 isoforms are required for maximal proliferation.

The eIF4A Inhibitor Silvestrol Potently Suppresses MPNST and VS Cell Proliferation and Induces G_2/M Arrest

To identify compounds with strong antiproliferative activity against VS and MPNSTs, we screened a panel of 23 natural

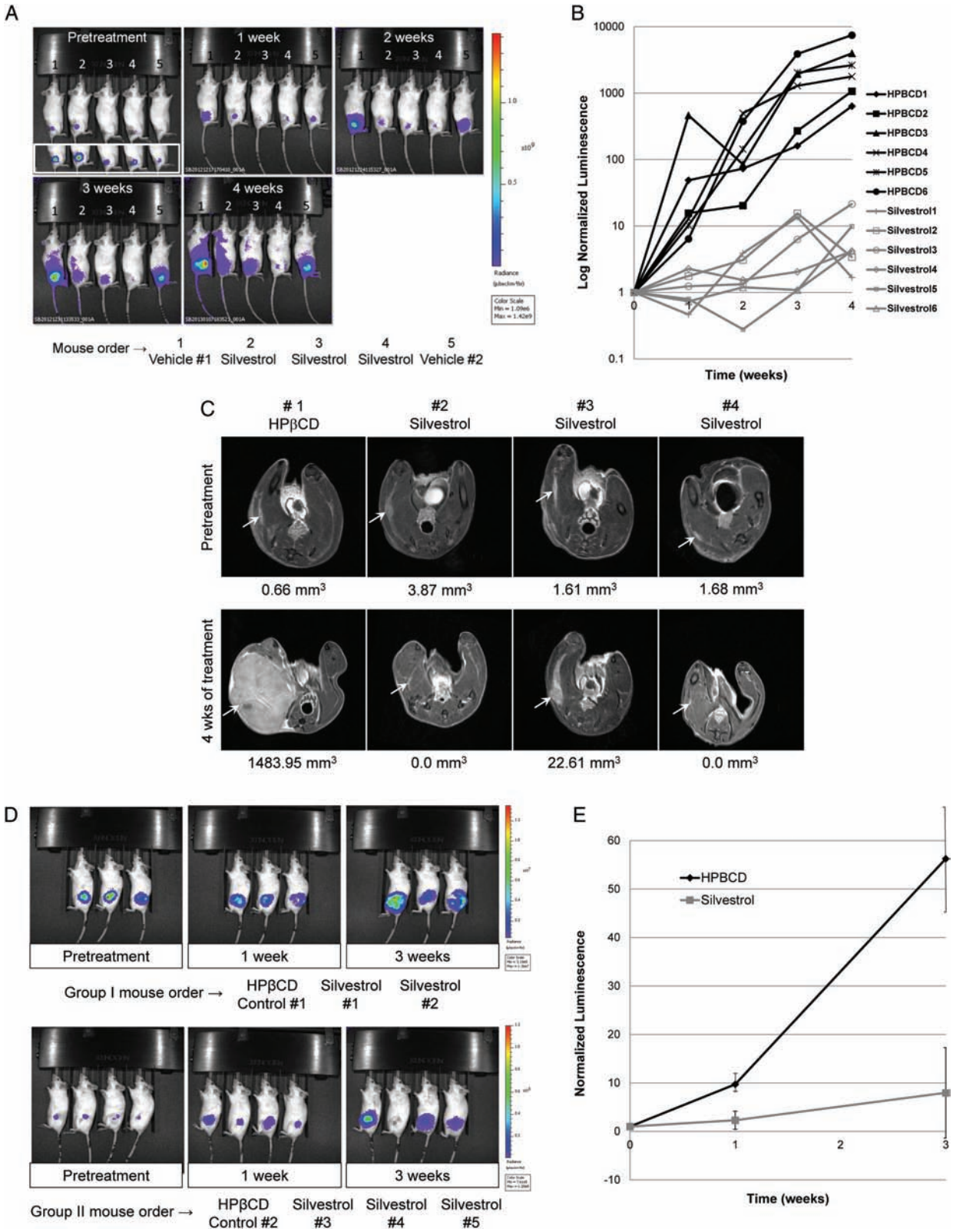

Fig. 5. Silvestrol potently suppresses the growth of orthotopic ST8814-Luc malignant peripheral nerve sheath tumor (MPNST) xenografts and Sch10545-Luc schwannoma allografts. (A) Shown are representative BL images of ST8814-Luc MPNST-bearing mice treated with silvestrol or HPβCD vehicle for the indicated weeks. The inset below the first panel was acquired using a lower threshold of bioluminescence detection, showing that all mice had established tumor prior to treatment. Note that silvestrol-treated mice showed a substantial decrease in BL signals.

compounds (Supplementary Table S2) in primary human Schwann and VS cells, *Nf2*$^{-/-}$ mouse schwannoma Sch10545 cells, and STS26T and ST8814 MPNST cells. Curiously, silvestrol, which targets the eIF4A1/2 helicase activity,[28] was identified as the most potent agent with an IC_{50} value of ~15 nM in VS cells compared with 40 nM in Schwann cells (Supplementary Table S6 and Supplementary Fig. S2). Likewise, silvestrol potently inhibited the growth of STS26T cells at ~10 nM of IC_{50} and ST8814 cells at ~40 nM of IC_{50} (Supplementary Fig. S2A). In addition, silvestrol suppressed mouse Sch10545 cells at slightly higher concentrations (Supplementary Table S6). Flow cytometry analysis revealed that ST8814 and STS26T MPNST and VS cells treated with 1 or 2 IC_{50} doses of silvestrol exhibited a substantial increase in the G_2/M population (Fig. 3A). A sub-G_1 fraction, suggestive of cell death, was notably increased in silvestrol-treated cells, particularly at the 2 IC_{50} dose. Consistently, phase contrast micrographs taken from these cells immediately before harvesting for cell cycle analysis showed decreased cell density and increased numbers of rounded and floating dead cells in silvestrol-treated dishes (Fig. 3B). Collectively, these results suggest that silvestrol potently inhibits proliferation of MPNST and VS cells by inducing cell cycle arrest at G_2/M.

Silvestrol Decreases the Levels of Several Cell-cycle Proteins and Upstream Signaling Kinases

To examine the mechanism underlying silvestrol-induced cell cycle arrest, we analyzed expression of several cell-cycle proteins. As cyclins D and E have been implicated to be controlled in part by protein translation,[27,29] we profiled various cyclin proteins expressed in the cell cycle. Interestingly, silvestrol treatment induced significant reductions in cyclins D1, E1, A, and B1 in STS26T and ST8814 MPNST and Sch10545 schwannoma cells (Fig. 4A). We also observed decreased protein levels of the Aurora A kinase in silvestrol-treated cells. In addition, the S-phase protein PCNA was markedly reduced in STS26T and Sch10545 cells.

As MPNSTs and VSs frequently exhibit abnormal activation of AKT, ERK1/2, and FAK,[11,30] which are important drivers for cell proliferation, we examined their expression following silvestrol treatment. In both STS26T and ST8814 MPNST cells and Sch10545 schwannoma cells, silvestrol induced a dose-dependent reduction in the total AKT and p-AKT levels as well as the total and phosphorylated protein levels of its downstream substrate PRAS40 (Fig. 4B). Also, silvestrol reduced the expression of the FAK protein in MPNST and Sch10545 cells. In addition, we observed a decrease in the protein levels of total ERK1/2 and p-ERKs in ST8814 and Sch10545 cells (Supplementary Fig. S3). These results suggest that silvestrol-induced cell-cycle arrest may be mediated in part by concurrently inhibiting the expression of multiple cyclins and mitogenic kinases.

Silvestrol Strongly Suppresses Tumor Growth in Orthotopic NF1$^{-/-}$ *MPNST and Nf2*$^{-/-}$ *Schwannoma Models*

To evaluate the antitumor efficacy of silvestrol, we established tumor-bearing mice by implanting luciferase-expressing *NF1*$^{-/-}$ ST8814 MPNST or *Nf2*$^{-/-}$ Sch10545 schwannoma cells into the sciatic nerves of SCID mice and used BLI to monitor tumor growth. ST8814-Luc tumor-bearing mice, when treated with HPβCD as the vehicle control, exhibited steady and rapid increases in tumor bioluminescence over time (Fig. 5A and B). In contrast, tumor-bearing mice treated with 1.5 mg/kg of silvestrol showed an average of 99% reduction in tumor size (Fig. 5B and Supplementary Fig. S4). Volumetric measurement by MRI confirmed our BLI results (Fig. 5C), although BLI appeared to be more sensitive at detecting residual tumor cells (Supplementary Table S7). Note that silvestrol was well-tolerated at the 1.5 mg/kg dose, with no overt weight loss in mice treated for 4 weeks (consistent with previous observations).[18] Similarly, we also observed that silvestrol treatment resulted in an average of 85% reduction in Sch10545-Luc schwannoma size compared with the vehicle control (Fig. 5D and E).

Histological staining of ST8814-Luc tumor sections showed that the silvestrol-treated tumors exhibited less cellularity and that the treated cells had nuclei with prominent chromatin condensation, reminiscent of pyknosis (Fig. 6A). These pyknotic nuclei indicate the sign of cell death.[31] TUNEL staining confirmed that silvestrol induced a nearly 6-fold increase in apoptotic cells in treated MPNST tumors. Immunostaining revealed that silvestrol-treated cells had a marked increase in the number of phospho-histone H3-positive cells, consistent with our in vitro data showing both G_2/M arrest and decreased Aurora A in silvestrol-treated cells (Figs 3A and 4A). Similarly, silvestrol-treated Sch10545-Luc tumors showed less cellularity and increased TUNEL labeling (Fig. 6B).

Taken together, these results indicate that silvestrol possesses potent antitumor effects in *NF1*$^{-/-}$ MPNSTs and *Nf2*$^{-/-}$ schwannomas.

Discussion

Overexpression of eIF4A, eIF4E, or eIF4G is often oncogenic and has been hypothesized to support the high protein synthesis rates in tumor cells.[2] We found that these eIF4F components are frequently overexpressed in both MPNSTs and VSs and confirmed that depleting eIF4A or eIF4E reduces cell growth. These results suggest that pharmacological targeting of the eIF4F complex might be a viable strategy for treating these tumors. Consistent with this notion, we have identified the eIF4A inhibitor silvestrol as a potent antitumor agent in MPNSTs and VSs.

High levels of eIF4F components in breast and hepatocellular carcinomas correlate with tumor progression and poor prognosis.[2,3] With the small number of tumors examined, we were

(B) Normalized luminescence from control HPβCD-treated (black lines) and silvestrol-treated (gray lines) ST8814-Luc xenografts ($n = 6$ per group). (C) MR images of ST8814-Luc xenografts at the beginning and end of treatment confirmed that silvestrol strongly suppresses tumor growth. (D) SCID mice bearing Sch10545-Luc schwannoma allografts were treated with silvestrol or HPβCD for 3 weeks. BLI showed that silvestrol also potently reduced schwannoma growth. (E) Mean normalized tumor luminescence signals with SDs in silvestrol- or HPβCD-treated mice bearing Sch10545-Luc schwannoma allografts are shown.

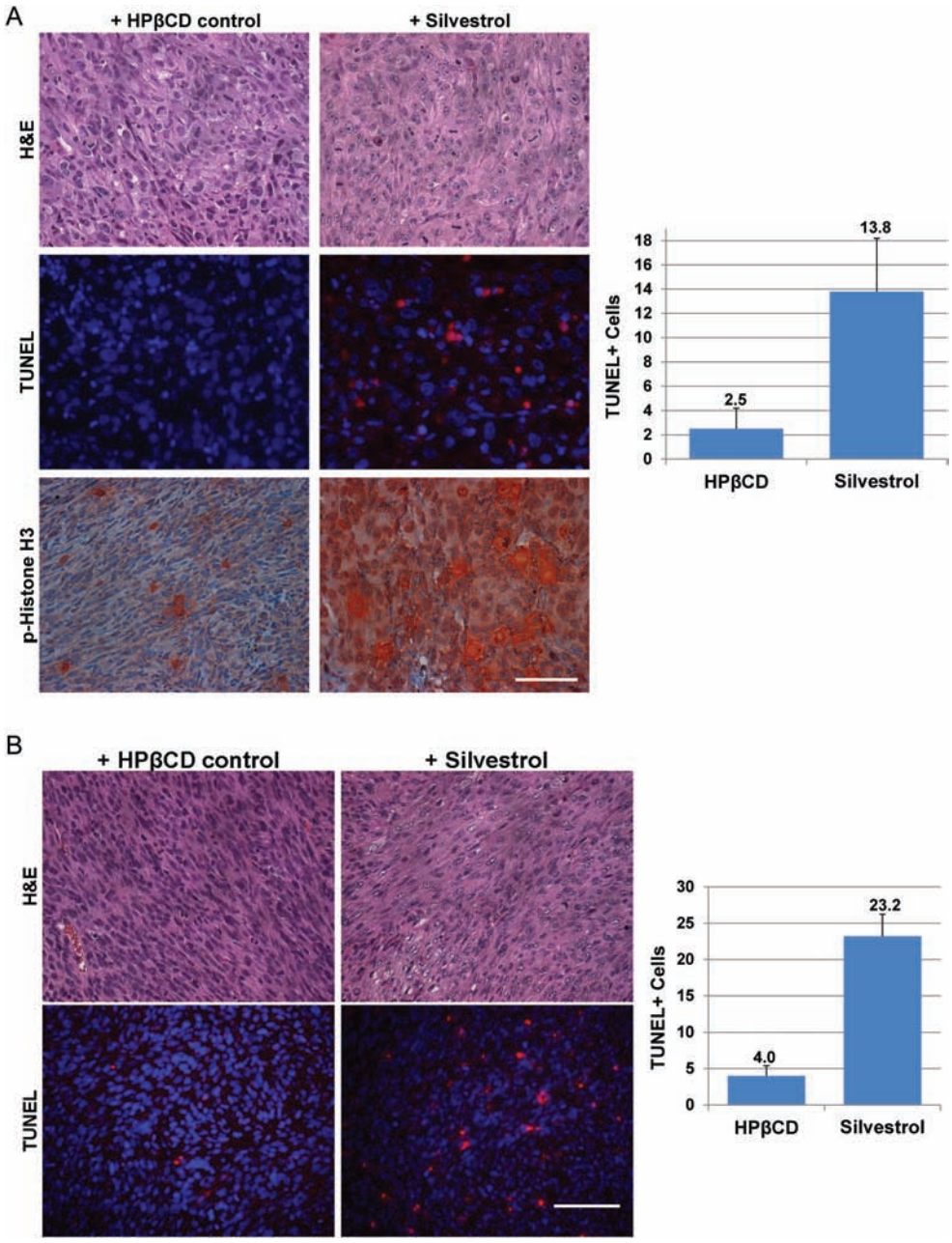

Fig. 6. Silvestrol-treated tumors exhibit decreased cellularity and increased apoptosis. (A) ST8814-Luc tumors treated with silvestrol for 4 weeks exhibited reduced cellularity (top) and increased TUNEL labeling (middle) and phospho-histone H3 staining (bottom) compared to HPβCD-treated controls. (B) Sch10545-Luc schwannomas treated with silvestrol for 3 weeks had reduced cellularity (top) and increased TUNEL labeling (bottom). Representative images are shown, and TUNEL-positive cells were counted from 2 or more fields with means and SDs calculated. Scale bar is 200 μm.

unable to find a statistically significant association between the expression of the eIF4F components and clinicopathological parameters in MPNSTs or VS. Interestingly, however, we observed that NF1-related MPNSTs appeared more likely to have stronger eIF4G staining than sporadic tumors. Likewise, NF2-associated and cystic-type VS tended to express higher eIF4A and eIF4E levels compared with non-NF2 and solid-type tumors, respectively. A recent study showed that large NF2-associated VS often exhibit more pronounced ribosomal protein S19 expression compared with small VSs, suggesting higher rates of protein synthesis in large tumors.[32] More comprehensive studies with larger sample sizes of MPNSTs and VS are therefore needed to validate our findings.

As in patient tumors, cultured MPNST cells also overexpressed eIF4F components compared with normal Schwann cells. Consistently, silencing of either eIF4A or eIF4E substantially reduced MPNST cell growth, indicating the importance of the eIF4F assembly in maintaining tumor cell proliferation.

Interestingly, we found that both eIF4A1 and eIF4A2 were important for MPNST cell proliferation as reducing either isoform significantly impeded cell growth. Also, eIF4A2 loss could not be compensated by the more abundant eIF4A1 isoform. Likewise, the increase in eIF4A2 expression after eIF4A1 knockdown did not rescue cell proliferation. The eIF4A2 isoform has been implicated in the promotion of cap-dependent translation[33] but its role in cell growth has not been defined.[34] More study is needed to further understand the functions of these 2 eIF4A isoforms in protein translation of MPNST and VS cells.

Currently, an FDA-approved medical therapy for MPNSTs or VS is not available. The highly invasive nature of MPNSTs makes complete surgical removal rare and contributes to the poor survival rate of these tumors. Patients with VS have a risk of perioperative complications such as cerebral hemorrhage or cerebrospinal fluid leak along with profound deafness and facial paralysis. Radiotherapy may introduce oncogenic mutations in these tumors. Efforts to develop a medical therapy for MPNST or VS have been made but with limited success. For example, RTK inhibition using erlotinib shows little clinical benefit for VS.[35,36] In the case of VEGF inhibition by bevacizumab, about 50% of VS patients exhibit tumor regression and hearing improvement[36]; however, there is a renewed tumor growth if it is necessary to discontinue treatment due to adverse effects. Also, the prolonged use of kinase inhibitors frequently activates alternative signaling pathways, conferring drug resistance. Additional targeted therapies and drug combinations are under evaluation as potential treatments for these tumors.

Drugs that target protein synthesis have been used for cancer treatment. Omacetaxine mepesuccinate (Synribo) is a plant-derived alkaloid that binds to the 60S ribosomal subunit, blocking peptide elongation.[37] Synribo is FDA-approved as a third-line treatment for chronic myelogenous leukemia resistant to RTK inhibitors.[38] The mTOR inhibitor rapamycin from *Streptomyces hygroscopicus* indirectly inactivates eIF4E, preventing its cap-binding ability. Rapamycin is used as an immunosuppressant to prevent organ transplant rejection and exhibits antiproliferative effects. The rapamycin-derivative everolimus is currently used as therapy for advanced renal cancer and pancreatic neuroendocrine tumors.[39,40] However, rapamycin and its derivatives are ineffective in VS patients and are cytostatic in MPNSTs.[41,42] Several other inhibitors of protein biosynthesis were also discovered as natural products. Cycloheximide from *Streptomyces griseus* blocks the elongation phase of protein synthesis. Due to severe adverse effects, cycloheximide is only used as an experimental tool. The marine natural product pateamine A inhibits eIF4A[3]; however, its high toxicity and difficulty in acquiring sufficient amounts have limited its drug development.

Silvestrol, first isolated from the tropical rainforest plant *Aglaia foveolata*, exhibits potent anticancer activity. Its full structure and absolute configuration have been established and confirmed by chemical synthesis.[13,15,43–45] Silvestrol is a reversible inhibitor of the eIF4A1/2 helicases, preventing the incorporation of eIF4A into the eIF4F cap-binding complex.[19,20] As a translational inhibitor, silvestrol has broader effects on tumor cells beyond those inhibitors targeting upstream signaling pathways such as AKT and ERKs. Indeed, we demonstrate that in addition to these 2 kinases, silvestrol reduces multiple cyclins, Aurora A, and FAK. Tumors often evade targeted therapies by re-activating PI3K/AKT and ERK signaling through alternative pathways. Silvestrol may prevent this mode of drug resistance since by inhibiting eIF4A, it reduces AKT levels in multiple cell types (as we and others have observed).[46] In addition, blocking eIF4F activity can reverse vemurafenib resistance in BRAF-mutant melanoma cells.[47]

Our observation that silvestrol treatment induced both G_2/M arrest and a profound reduction of multiple cyclins and kinases in both MPNST and VS cells is consistent with reports indicating that silvestrol causes rapid cyclin loss and subsequent cell cycle arrest.[14,21] As cyclins D and E are translationally regulated,[27,29] silvestrol may directly interfere with cyclin protein synthesis. Since tumor cells frequently abrogate the G_1 checkpoint, they maintain G_1 progression despite decreases in G_1 cyclins. Since the levels of the Aurora A kinase were substantially reduced by silvestrol, MPNST and VS cells would be expected to arrest in G_2/M. Alternatively, silvestrol may also activate the G_2/M checkpoint by promoting the generation of reactive oxygen species.[13] Furthermore, decreasing protein synthesis by silvestrol would likely trigger long-term changes in cell signaling over time. It has been shown that the silvestrol-related rocaglamide A decreases the activity of heat shock factor 1 (HSF1), a transcription factor important for cell metabolism, proliferation, and stress survival.[48] This decrease in HSF1 activity was observed with several classes of translational inhibitors, including cycloheximide. Thus, reduced HSF1-mediated transcription may be a general consequence of impeding protein synthesis. It is plausible that part of silvestrol's antitumor activity is due to a blockade in HSF1-mediated transcription, making treated tumors vulnerable to apoptosis.

In summary, our results identify the eIF4F complex as a potential drug target for both MPNSTs and VS, tumors that currently do not have effective chemotherapy. The eIF4A inhibitor silvestrol was selected from our natural compound screening as the most potent antitumor compound in both tumor types, validating eIF4F as a possible tumor target. As silvestrol was well-tolerated, these promising results indicate that silvestrol merits further exploration as a drug candidate for MPNSTs and VS.

Supplementary Material

Supplementary material is available at *Neuro-Oncology Journal* online (http://neuro-oncology.oxfordjournals.org/).

Funding

This study was supported by grants from Advocure NF2, Galloway Family Fund, Meningioma Mommas, the Research Institute at Nationwide Children's Hospital (to L.S.C.), Children's Tumor Foundation, NF Midwest (to D.B.W. and L.S.C.), and National Cancer Institute (P01 CA125066 to A.D.K. and P30 CA16058 to The OSU Comprehensive Cancer Center).

Acknowledgments

We sincerely thank Steven Carroll for the ST8814-Luc cells; Kimerly Powell and the Small-Animal Imaging Core, the OSU Cooperative Human Tissue Network and Tissue Archives for tumor specimens; Joseph Stanek of the NCH Center for Innovation in Pediatric Practice for statistical analysis; and Timothy Cripe for critical reading of the manuscript.

Conflict of interest statement. None declared.

References

1. Jackson RJ, Hellen CU, Pestova TV. The mechanism of eukaryotic translation initiation and principles of its regulation. *Nat Rev Mol Cell Biol*. 2010;11(2):113–127.
2. Silvera D, Formenti SC, Schneider RJ. Translational control in cancer. *Nat Rev Cancer*. 2010;10(4):254–266.
3. Bhat M, Robichaud N, Hulea L, et al. Targeting the translation machinery in cancer. *Nat Rev Drug Discov*. 2015;14(4):261–278.
4. Modelska A, Turro E, Russell R, et al. The malignant phenotype in breast cancer is driven by eIF4A1-mediated changes in the translational landscape. *Cell Death Dis*. 2015;6:e1603.
5. Wolfe AL, Singh K, Zhong Y, et al. RNA G-quadruplexes cause eIF4A-dependent oncogene translation in cancer. *Nature*. 2014; 513(7516):65–70.
6. Katz D, Lazar A, Lev D. Malignant peripheral nerve sheath tumour (MPNST): the clinical implications of cellular signalling pathways. *Expert Rev Mol Med*. 2009;11:e30.
7. Bollag G, Clapp DW, Shih S, et al. Loss of NF1 results in activation of the Ras signaling pathway and leads to aberrant growth in haematopoietic cells. *Nat Genet*. 1996;12(2):144–148.
8. Brems H, Beert E, de Ravel T, Legius E. Mechanisms in the pathogenesis of malignant tumours in neurofibromatosis type 1. *Lancet Oncol*. 2009;10(5):508–515.
9. Rouleau GA, Merel P, Lutchman M, et al. Alteration in a new gene encoding a putative membrane-organizing protein causes neuro-fibromatosis type 2. *Nature*. 1993;363(6429):515–521.
10. Trofatter JA, MacCollin MM, Rutter JL, et al. A novel moesin-, ezrin-, radixin-like gene is a candidate for the neurofibromatosis 2 tumor suppressor. *Cell*. 1993;72(5):791–800.
11. Bush ML, Oblinger J, Brendel V, et al. AR42, a novel histone deacetylase inhibitor, as a potential therapy for vestibular schwannomas and meningiomas. *Neuro Oncol*. 2011;13(9): 983–999.
12. Scoles DR, Yong WH, Qin Y, Wawrowsky K, Pulst SM. Schwannomin inhibits tumorigenesis through direct interaction with the eukaryotic initiation factor subunit c (eIF3c). *Hum Mol Genet*. 2006;15(7):1059–1070.
13. Lucas DM, Edwards RB, Lozanski G, et al. The novel plant-derived agent silvestrol has B-cell selective activity in chronic lymphocytic leukemia and acute lymphoblastic leukemia in vitro and in vivo. *Blood*. 2009;113(19):4656–4666.
14. Alinari L, Prince CJ, Edwards RB, et al. Dual targeting of the cyclin/ Rb/E2F and mitochondrial pathways in mantle cell lymphoma with the translation inhibitor silvestrol. *Clin Cancer Res*. 2012; 18(17):4600–4611.
15. Pan L, Kardono LB, Riswan S, et al. Isolation and characterization of minor analogues of silvestrol and other constituents from a large-scale re-collection of *Aglaia foveolata*. *J Nat Prod*. 2010; 73(11):1873–1878.
16. Kogure T, Kinghorn AD, Yan I, et al. Therapeutic potential of the translation inhibitor silvestrol in hepatocellular cancer. *PLoS One*. 2013;8(9):e76136.
17. Wiegering A, Uthe FW, Jamieson T, et al. Targeting Translation Initiation Bypasses Signaling Crosstalk Mechanisms That Maintain High MYC Levels in Colorectal Cancer. *Cancer Discov*. 2015;5(7):768–781.
18. Saradhi UV, Gupta SV, Chiu M, et al. Characterization of silvestrol pharmacokinetics in mice using liquid chromatography-tandem mass spectrometry. *AAPS J*. 2011;13(3):347–356.
19. Chambers JM, Lindqvist LM, Webb A, et al. Synthesis of biotinylated episilvestrol: highly selective targeting of the translation factors eIF4AI/II. *Org Lett*. 2013;15(6):1406–1409.
20. Sadlish H, Galicia-Vazquez G, Paris CG, et al. Evidence for a Functionally Relevant Rocaglamide Binding Site on the eIF4A-RNA Complex. *ACS Chem Biol*. 2013;8(7):1519–1527.
21. Cencic R, Carrier M, Galicia-Vázquez G, et al. Antitumor activity and mechanism of action of the cyclopenta[b]benzofuran, silvestrol. *PLoS One*. 2009;4(4):e5223.
22. Bush ML, Burns SS, Oblinger J, et al. Treatment of Vestibular Schwannoma Cells With ErbB Inhibitors. *Otol Neurotol*. 2012; 33(2):244–257.
23. Kinghorn AD, Pan L, Fletcher JN, Chai H. The relevance of higher plants in lead compound discovery programs. *J Nat Prod*. 2011; 74(6):1539–1555.
24. Burns SS, Akhmametyeva EM, Oblinger JL, et al. Histone deacetylase inhibitor AR-42 differentially affects cell-cycle transit in meningeal and meningioma cells, potently inhibiting NF2-deficient meningioma growth. *Cancer Res*. 2013;73(2):792–803.
25. Turk AN, Byer SJ, Zinn KR, Carroll SL. Orthotopic xenografting of human luciferase-tagged malignant peripheral nerve sheath tumor cells for in vivo testing of candidate therapeutic agents. *J Vis Exp*. 2011;49:e2558.
26. Chang LS, Jacob A, Abraham J, et al. Growth of benign and malignant schwannoma xenografts in severe combined immunodeficiency mice. *Laryngoscope*. 2006;116(11):2018–2026.
27. Rosenwald IB, Kaspar R, Rousseau D, et al. Eukaryotic translation initiation factor 4E regulates expression of cyclin D1 at transcriptional and post-transcriptional levels. *J Biol Chem*. 1995; 270(36):21176–21180.
28. Bordeleau ME, Robert F, Gerard B, et al. Therapeutic suppression of translation initiation modulates chemosensitivity in a mouse lymphoma model. *J Clin Invest*. 2008;118(7):2651–2660.
29. Lai MC, Chang WC, Shieh SY, Tarn WY. DDX3 regulates cell growth through translational control of cyclin E1. *Mol Cell Biol*. 2010; 30(22):5444–5453.
30. Poulikakos PI, Xiao GH, Gallagher R, et al. Re-expression of the tumor suppressor NF2/merlin inhibits invasiveness in mesothelioma cells and negatively regulates FAK. *Oncogene*. 2006;25(44):5960–5968.
31. Burgoyne LA. The mechanisms of pyknosis: hypercondensation and death. *Exp Cell Res*. 1999;248(1):214–222.
32. Mehrian-Shai R, Freedman S, Shams S, et al. Schwannomas exhibit distinct size-dependent gene-expression patterns. *Future Oncol*. 2015;11(12):1751–1758.
33. Fukao A, Mishima Y, Takizawa N, et al. MicroRNAs trigger dissociation of eIF4AI and eIF4AII from target mRNAs in humans. *Mol Cell*. 2014;56(1):79–89.
34. Galicia-Vázquez G, Cencic R, Robert F, Agenor AQ, Pelletier J. A cellular response linking eIF4AI activity to eIF4AII transcription. *RNA*. 2012;18(7):1373–1384.
35. Plotkin SR, Halpin C, McKenna MJ, et al. Erlotinib for progressive vestibular schwannoma in neurofibromatosis 2 patients. *Otol Neurotol*. 2010;31(7):1135–1143.
36. Plotkin SR, Merker VL, Halpin C, et al. Bevacizumab for progressive vestibular schwannoma in neurofibromatosis type 2: a retrospective review of 31 patients. *Otol Neurotol*. 2012;33(6): 1046–1052.
37. Robert F, Carrier M, Rawe S, et al. Altering chemosensitivity by modulating translation elongation. *PLoS One*. 2009;4(5):e5428.

38. Gandhi V, Plunkett W, Cortes JE. Omacetaxine: a protein translation inhibitor for treatment of chronic myelogenous leukemia. *Clin Cancer Res*. 2014;20(7):1735–1740.
39. Motzer RJ, Escudier B, Oudard S, et al. Efficacy of everolimus in advanced renal cell carcinoma: a double-blind, randomised, placebo-controlled phase III trial. *Lancet*. 2008;372(9637):449–456.
40. Panzuto F, Rinzivillo M, Fazio N, et al. Real-world study of everolimus in advanced progressive neuroendocrine tumors. *Oncologist*. 2014;19(9):966–974.
41. Johannessen CM, Reczek EE, James MF, et al. The NF1 tumor suppressor critically regulates TSC2 and mTOR. *Proc Natl Acad Sci USA*. 2005;102(24):8573–8578.
42. Giovannini M, Bonne NX, Vitte J, et al. mTORC1 inhibition delays growth of neurofibromatosis type 2 schwannoma. *Neuro Oncol*. 2014;16(4):493–504.
43. Hwang BY, Su BN, Chai H, et al. Silvestrol and episilvestrol, potential anticancer rocaglate derivatives from *Aglaia silvestris*. *J Org Chem*. 2004;69(10):3350–3358.
44. Kim S, Hwang BY, Su BN, et al. Silvestrol, a potential anticancer rocaglate derivative from *Aglaia foveolata*, induces apoptosis in LNCaP cells through the mitochondrial/apoptosome pathway without activation of executioner caspase-3 or -7. *Anticancer Res*. 2007;27(4B):2175–2183.
45. Pan L, Woodard JL, Lucas DM, Fuchs JR, Kinghorn AD. Rocaglamide, silvestrol and structurally related bioactive compounds from Aglaia species. *Nat Prod Rep*. 2014;31(7):924–939.
46. Patton JT, Lustberg ME, Lozanski G, et al. The translation inhibitor silvestrol exhibits direct anti-tumor activity while preserving innate and adaptive immunity against EBV-driven lymphoproliferative disease. *Oncotarget*. 2015;6(5):2693–2708.
47. Boussemart L, Malka-Mahieu H, Girault I, et al. eIF4F is a nexus of resistance to anti-BRAF and anti-MEK cancer therapies. *Nature*. 2014;513(7516):105–109.
48. Santagata S, Mendillo ML, Tang YC, et al. Tight coordination of protein translation and HSF1 activation supports the anabolic malignant state. *Science*. 2013;341(6143):1238303.